Radiating Instabilities of Internal Inertio-Gravity Waves

FRANK KWASNIOK AND GERHARD SCHMITZ

Leibniz-Institut für Atmosphärenphysik, Kuehlungsborn, Germany

(Manuscript received 14 August 2001, in final form 9 December 2002)

ABSTRACT

The vertical radiation of local convective and shear instabilities of internal inertio-gravity waves is examined within linear stability theory. A steady, plane-parallel Boussinesq flow with vertical profiles of horizontal velocity and static stability resembling an internal inertio-gravity wave packet without mean vertical shear is used as the dynamical framework. The influence of primary wave frequency and amplitude, as well as orientation and horizontal wavenumber of the instability on vertical radiation, is discussed. Considerable radiation occurs at small to intermediate instability wavenumbers for basic-state gravity waves with high to intermediate frequencies and moderately convectively supercritical amplitudes. Radiation is then strongest when the horizontal wave vector of the instability is aligned parallel to the horizontal wave vector of the basic-state gravity wave. These radiating modes are essentially formed by shear instability. Convective instabilities, that occur at large instability wavenumbers or strongly convectively supercritical amplitudes, as well as shear instabilities of low-frequency basic-state gravity waves, are nonradiating, trapped in the region of instability. The radiation of an instability is found to be related to the existence of critical levels, a radiating mode being characterized by the absence of critical levels outside the region of instability of the primary wave.

1. Introduction

Numerous observational and theoretical studies have shown the importance of internal gravity waves in determining the circulation and structure of the atmosphere, particularly of the mesosphere. As internal gravity waves grow in amplitude when propagating upward, they may become unstable to local convective or shear instability [see Fritts and Rastogi (1985) for a review]. The latter is also referred to as dynamical or Kelvin–Helmholtz instability. These two mechanisms are commonly believed to play an important role in gravity wave saturation and breakdown and to contribute significantly to momentum deposition, the dissipation of larger-scale motions and the generation of turbulence in the mesosphere.

Instabilities of gravity waves have been subject of a variety of theoretical studies. Fritts and Yuan (1989) investigated the stability of the environment due to a large-amplitude inertio-gravity wave (IGW) using a hyperbolic tangent profile of horizontal velocity without mean vertical shear. The study has been extended to a situation with mean vertical shear by Yuan and Fritts (1989). A stability analysis that is similar to that of Fritts and Yuan (1989) has been performed by Dunkerton (1997), however, employing a wave packet as basic-state velocity profile, which seems to be more adequate than a hyperbolic tangent profile since the vertical structure of IGW is more sinusoidal rather than having the form of a simple shear layer. Complementary to such linear stability analyses, gravity wave instability has been investigated by direct numerical simulation (Winters and d'Asaro 1989; Walterscheid and Schubert 1990; Sutherland and Peltier 1994; Lelong and Dunkerton 1998a,b).

A particularly interesting and potentially important issue are radiating instabilities, that is, instabilities that result in waves being radiated vertically far from the seat of instability. Such radiating modes can grow to large amplitudes and may lead to the generation of turbulence even at height levels outside the region of instability of the primary gravity wave. The aspect of vertical radiation of instabilities has been addressed by means of linear stability analysis and nonlinear numerical simulation by Dunkerton and Robins (1992) for a gravity wave critical layer and by Sutherland et al. (1994) for a Bickley jet profile and a hyperbolic tangent profile.

The present study aims to give a systematic survey on radiating instabilities that arise from a realistic sinusoidal IGW basic state within linear stability theory. It is an extension of the papers by Dunkerton and Robins (1992), Sutherland et al. (1994), and Dunkerton (1997) regarding linear theory. It brings together and builds on ideas and results of these papers. The effectiveness of radiation of an instability is measured by the penetration

Corresponding author address: Dr. Frank Kwasniok, Dept. of Statistics, London School of Economics, Houghton Street, London WC2A 2AE, United Kingdom.
E-mail: f.kwasniok@lse.ac.uk

ratio (Sutherland et al. 1994) that quantifies the extent to which the linear eigenfunction penetrates from the region of instability into the adjacent stable regions of the wave field. The study is performed under the assumption of steady plane-parallel flow as is usually done. This assumption is justified if instabilities are investigated that are local compared to the horizontal wavelength of the primary gravity wave, and fast compared to the period of the primary gravity wave. The dependence of radiation upon IGW frequency and amplitude as well as orientation and horizontal wavenumber of instability is discussed.

The paper is organized as follows. In section 2, the theory of local instabilities in Boussinesq plane-parallel shear flows and their vertical radiation is recapitulated. Then the particular basic-state configuration relevant to IGW is introduced and the numerical solution of the corresponding eigenvalue problem is outlined. The results are illustrated and discussed in section 3. The paper closes with a short summarizing and concluding section.

2. Theory

a. Stability analysis

In the present study, we consider instabilities on a steady, plane-parallel, stratified shear flow in the Boussinesq approximation without dissipation and rotation with vertical profiles of horizontal velocity $u = u(z)$ and static stability $N^2 = N^2(z)$. As is well known, such a flow may give rise to growth of initial perturbations, a necessary condition for shear instability being that the mean Richardson number is below 0.25 somewhere in the flow (Miles 1961; Howard 1961). A convectively unstable situation is clearly characterized by a negative Richardson number. The nondivergent perturbation velocity field can be expressed in terms of a streamfunction $\Psi(x, z)$. A disturbance is assumed that is periodic in the horizontal direction with some wavenumber k, complex phase speed c, complex frequency $\omega = kc$, and an amplitude that varies with height: $\Psi(x, z) = \phi(z) \exp[ik(x - ct)]$. Within the framework of linear stability theory, the complex amplitude $\phi(z)$ then satisfies the Taylor–Goldstein equation (e.g., Drazin and Reid 1981):

$$\phi_{zz} + \gamma^2\phi = 0, \tag{1}$$

with

$$\gamma^2 = \frac{N^2}{(c - u)^2} + \frac{u_{zz}}{c - u} - k^2. \tag{2}$$

The subscript z denotes differentiation with respect to z. Having the application to an internal gravity wave packet in mind, we consider a flow that is unbounded below and above ($-\infty < z < \infty$), and for which below and above some level ($z < -\hat{z} < 0$ and $0 < \hat{z} < z$) the horizontal velocity and the static stability are constant. Hereafter, the domain $-\hat{z} \le z \le \hat{z}$ is referred to as the center or inner region and the domains $z < -\hat{z}$ and $\hat{z} < z$ are referred to as the far-field or outer regions. If $u(z) = \hat{u}$ and $N^2(z) = \hat{N}^2$ for $\hat{z} < z$ (or $z < -\hat{z}$), then Eq. (1) becomes the familiar wave equation with solution

$$\phi(z) = C_+ \exp(i\hat{\gamma}z) + C_- \exp(-i\hat{\gamma}z), \tag{3}$$

where C_+ and C_- are complex constants and the vertical wavenumber $\hat{\gamma}$ is given by

$$\hat{\gamma}^2 = \frac{\hat{N}^2}{(c - \hat{u})^2} - k^2. \tag{4}$$

Anticipating the position of boundary conditions, the branch of the square root in the calculation of $\hat{\gamma}$ is taken so that

$$0 < \arg(\hat{\gamma}) \le \pi. \tag{5}$$

In the following, we assume that $\hat{u} = 0$ as is the case for the IGW velocity profile that will be introduced later. Physically meaningful solutions have the form of Eq. (3) with $C_- = 0$ (or $C_+ = 0$). This follows by requiring that $|\phi(z)|$ stays bounded as $z \to \infty$ (or $z \to -\infty$) when $\mathrm{Im}(\hat{\gamma}) \neq 0$ and by the requirement for upward energy propagation when $\mathrm{Im}(\hat{\gamma}) = 0$. It can be immediately seen that $\mathrm{Im}(\hat{\gamma}) \neq 0$ for an unstable mode [$\mathrm{Im}(c) > 0$]. It follows that all unstable modes have $|\phi(z)| \to 0$ as $z \to \pm\infty$. In this paper, we only deal with unstable modes.

b. Radiation of instabilities into the far-field regions

The question of how to assess the ability of a disturbance to radiate into the far-field regions has been debated in the literature. The most natural approach is to look how rapidly the eigenfunction $\phi(z)$ decays in the outer regions. However, McIntyre and Weissman (1978) put forward doubts if the extent to which the linear eigenfunction appears to penetrate into the far-field regions is a reliable measure of the effectiveness of radiation. They conjecture that the penetration depth may merely reflect the growth rate of the instability. Instead, they propose the phase speed condition for sustained radiation, requiring that $|\mathrm{Re}(\omega)| < \hat{N}$ (in the case $\hat{u} = 0$) as a classification within linear theory. It is based on the reasoning that sustained radiation will be favored when the real part of the phase speed of the instability matches the phase speed of some possible freely propagating wave with the same horizontal wavelength. Moreover, McIntyre and Weissman (1978) advocate a nonlinear treatment of the problem to answer the question of whether or not the phase speed condition is satisfied since a mature stage of the disturbance involving nonlinear processes may be dominated by phase speeds or wavelengths different from those of the linear stage. Especially for strong instabilities, they consider linear theory unreliable.

On the other hand, the work by Sutherland et al. (1994) seems to allow more optimism concerning linear theory. They introduce the penetration ratio $\mathrm{Re}(\hat{\gamma})/\mathrm{Im}(\hat{\gamma})$ as a

measure of the intrusion of an instability into the far-field regions. The penetration ratio is the ratio of the length scale on which the amplitude of the instability decreases by a factor e to the wavelength of the instability. Sutherland et al. (1994) discuss the dependence of the penetration ratio on the complex instability frequency ω. The absolute penetration ratio decreases with increasing growth rate, especially $|\mathrm{Re}(\hat{\gamma})/\mathrm{Im}(\hat{\gamma})| < 1$ whenever $\mathrm{Im}(\omega) > \hat{N}/\sqrt{8}$, but it also depends substantially on the real part of instability frequency. For an instability of a given growth rate $\mathrm{Im}(\omega)$, the absolute penetration ratio is largest if $[\mathrm{Re}(\omega)]^2 = (1/3)(\hat{N}^2 + [\mathrm{Im}(\omega)]^2)$. The penetration ratio exhibits a cutoff when the real part of instability frequency exceeds the background Brunt–Väisälä frequency: $|\mathrm{Re}(\hat{\gamma})/\mathrm{Im}(\hat{\gamma})| < 1$ whenever $|\mathrm{Re}(\omega)| > \hat{N}$. This is in accordance with the phase speed condition of McIntyre and Weissman (1978). Moreover, Sutherland et al. (1994) show by a couple of representative nonlinear simulations that the penetration ratio derived from only linear theory does indeed correctly predict the effectiveness of wave radiation.

Having all this in mind, we believe that linear stability theory can provide useful information on radiation of IGW basic-state instability. We therefore stick to linear theory in the present study and regard the far-field structure of a growing eigenfunction obtained from linear stability theory characterized by the penetration ratio as an indicator of the capability of this instability to radiate.

c. IGW basic-state configuration

For this study, vertical profiles of horizontal velocity and static stability resembling an inertio-gravity wave packet are adopted (cf. Dunkerton 1997):

$$u = ac_0A(\cos m_0 z \cos\alpha + R \sin m_0 z \sin\alpha), \quad (6)$$

$$N^2 = N_0^2(1 - aA \cos m_0 z). \quad (7)$$

The envelope of the wave packet is

$$A = A(z) = \exp\left[-\left(\frac{z}{\sigma}\right)^2\right]. \quad (8)$$

Here, $R = f/\omega_0$ is a nondimensional rotation rate, f being the Coriolis parameter and ω_0 being the IGW intrinsic frequency. The phase of IGW is $m_0 z$ in the approximation of steady plane-parallel flow. Without loss of generality, the IGW horizontal wave vector points in the x direction; α is the azimuthal angle between the horizontal wave vectors of IGW and instability; u then is the component of the horizontal velocity field parallel to the instability wave vector. The phase speed c_0 and the vertical wavenumber m_0 of IGW are related through the dispersion relation for hydrostatic IGW:

$$m_0^2 = \frac{N_0^2}{c_0^2(1 - R^2)}. \quad (9)$$

Parameter a is a nondimensional wave amplitude such that $a = 1$ corresponds to a convectively neutral situation. The form of the envelope is different from that of Dunkerton (1997). Since our main concern is the far-field structure of the eigenfunctions, it is necessary to use profiles of horizontal velocity and static stability that are smooth everywhere; discontinuities may cause spurious modes.

An analysis of the profile of Richardson number corresponding to the IGW basic state considered here as performed by Dunkerton (1997) reveals for which convectively stable IGW configurations ($a < 1$) shear instability is possible. In the case of transverse instability ($\alpha = 90°$), for all $0 < R < 1$ there is an IGW amplitude $a < 1$ so that $\mathrm{Ri} < 0.25$. When $\alpha < 90°$, larger amplitudes are required at any value of R in order to attain $\mathrm{Ri} < 0.25$. For parallel instability ($\alpha = 0°$), R has to exceed $1/\sqrt{2}$ to reach $\mathrm{Ri} < 0.25$ for convectively subcritical amplitudes. However, the condition $\mathrm{Ri} < 0.25$ is not sufficient for shear instability, nor is the depression of Ri below 0.25 by itself a good indicator of growth rate. Other factors in addition to Ri determine the growth rate. It has been shown by Fritts and Yuan (1989) for a hyperbolic tangent profile, and by Dunkerton (1997) for a wave packet, that without mean vertical shear even for $\alpha = 90°$, significant shear instability of a convectively stable basic state occurs only for R larger than about 0.7.

Nondimensional quantities are introduced as $z_* = m_0 z$, $k_* = k/m_0$, $\gamma_* = \gamma/m_0$, $c_* = c/c_0$, and $u_* = u/c_0$. Insertion of Eqs. (6) and (7) into Eq. (1) using the dispersion relation of Eq. (9) yields

$$\phi_*'' + \gamma_*^2 \phi_* = 0, \quad (10)$$

with

$$\gamma_*^2 = \frac{(1 - R^2)(1 - aA \cos z_*)}{(c_* - u_*)^2} + \frac{u_*''}{c_* - u_*} - k_*^2. \quad (11)$$

The prime denotes differentiation with respect to z_*; ϕ_* denotes a nondimensional streamfunction amplitude; the nondimensionalization is arbitrary since any eigenfunction is only determined up to a factor anyway. The eigenvalue problem depends in a nontrivial manner on nondimensional rotation rate R, IGW amplitude a, instability orientation α, nondimensional instability horizontal wavenumber k_*, and localization parameter σ. A variation of the phase speed c_0 of the basic-state gravity wave results only in a linear scaling of the instability wavenumber k, and a variation of the background static stability N_0^2 results only in a linear scaling of the complex instability frequency ω. It follows from Eqs. (6) and (7) that $u_* \to \hat{u}_* = 0$ and $N^2 \to \hat{N}^2 = N_0^2$ as $z_* \to \pm\infty$. The nondimensional vertical wavenumber of the instability in the far-field regions is thus given by

$$\hat{\gamma}_*^2 = \frac{1 - R^2}{c_*^2} - k_*^2. \quad (12)$$

The penetration ratio characterizing the far-field struc-

ture of the eigenfunctions is here (different from Sutherland et al. 1994) defined as

$$D = \frac{1}{2\pi}\frac{\mathrm{Re}(\hat{\gamma}_*)}{\mathrm{Im}(\hat{\gamma}_*)}, \tag{13}$$

so that a value $|D| = 1$ really means that the amplitude of the eigenfunction decreases by a factor e within a wavelength. Because of $\hat{u}_* = 0$ we always have $D \leq 0$ as can be readily seen from a mathematical discussion of $\hat{\gamma}_*^2$ and $\hat{\gamma}_*$. Physically, this corresponds to energy propagation from the inner region into the outer regions.

The eigenvalue problem has special properties for some particular values of the parameters arising from certain symmetries: First, if $R = 0$ or $\alpha = 0°$, the profile of horizontal velocity is symmetric with respect to the center: $u_*(-z_*) = u_*(z_*)$. It follows that $\gamma_*^2(-z_*) = \gamma_*^2(z_*)$ for arbitrary c_* and thus any eigenfunction is symmetric: $\phi_*(-z_*) = \phi_*(z_*)$. Second, for $\alpha = 90°$, u_* is antisymmetric: $u_*(-z_*) = -u_*(z_*)$. If, additionally, $\mathrm{Re}(c_*) = 0$ (as turns out to be always the case for the most unstable mode), it follows that $\gamma_*^2(-z_*) = \overline{\gamma_*^2(z_*)}$ where the overbar denotes the complex conjugate; corresponding eigenfunctions then fulfill $\phi_*(-z_*) = \overline{\phi_*(z_*)}$. Moreover, $\hat{\gamma}_*^2$ is then purely real and negative [Eq. (12)] and thus $\hat{\gamma}_*$ is purely imaginary. Hence such modes have $D = 0$; that is, they are nonradiating.

d. Numerical solution of the eigenvalue problem

The algorithm employed to solve the eigenvalue problem is essentially a kind of shooting method. The boundary conditions demanding that $|\phi_*(z_*)|$ is bounded as $z_* \to \pm\infty$ are represented by radiation boundary conditions applied at positions $-\hat{z}_* < 0$ and $\hat{z}_* > 0$:

$$\phi_*'(-\hat{z}_*) = -i\hat{\gamma}_*\phi_*(-\hat{z}_*), \tag{14}$$

$$\phi_*'(\hat{z}_*) = i\hat{\gamma}_*\phi_*(\hat{z}_*). \tag{15}$$

Introducing the vector of real variables $\mathbf{y} = (y_1, y_2, y_3, y_4)^{\mathrm{T}}$ with $y_1 = \mathrm{Re}(\phi_*)$, $y_2 = \mathrm{Im}(\phi_*)$, $y_3 = \mathrm{Re}(\phi_*')$, and $y_4 = \mathrm{Im}(\phi_*')$, Eq. (10) can be written as a nonautonomous dynamical system of first order:

$$y_1' = y_3, \tag{16}$$

$$y_2' = y_4, \tag{17}$$

$$y_3' = -\mathrm{Re}(\gamma_*^2)y_1 + \mathrm{Im}(\gamma_*^2)y_2, \tag{18}$$

$$y_4' = -\mathrm{Im}(\gamma_*^2)y_1 - \mathrm{Re}(\gamma_*^2)y_2. \tag{19}$$

An eigenfunction is only determined up to an arbitrary complex factor. Thus, without loss of generality, one can assume $y_1(0) = 1$ and $y_2(0) = 0$. The dynamical system of Eqs. (16)–(19) is integrated backward from $z_* = 0$ to $z_* = -\hat{z}_*$ and forward from $z_* = 0$ to $z_* = \hat{z}_*$ with initial condition $\mathbf{y}(0) = [1, 0, y_3(0), y_4(0)]^{\mathrm{T}}$. A cost function is introduced that measures the violation of the radiation boundary conditions:

$$\begin{aligned}\chi^2 &= \chi^2[\mathrm{Re}(c_*), \mathrm{Im}(c_*), y_3(0), y_4(0); \hat{z}_*] \\ &= |\phi_*'(-\hat{z}_*) + i\hat{\gamma}_*\phi_*(-\hat{z}_*)|^2 \\ &\quad + |\phi_*'(\hat{z}_*) - i\hat{\gamma}_*\phi_*(\hat{z}_*)|^2.\end{aligned} \tag{20}$$

It depends on the complex phase speed c_*, the complex slope of the function ϕ_* at zero, and the real parameter $\hat{z}_*$. The complex phase speed and the eigenfunction are determined simultaneously by minimizing the cost function. For a solution of the eigenvalue problem, the value of the cost function at the minimum has to be zero (up to numerical error). It is important to note that the radiation boundary conditions select the solution that is bounded as $z_* \to \pm\infty$ only when applied at a position $\hat{z}_*$ where the solution has already attained its far-field behavior given by Eq. (3). Hence it is essential to verify that $\hat{z}_*$ is chosen large enough. This can be done in the following way. Having found a zero value of the cost function at some complex phase speed c_* for a particular parameter value $\hat{z}_*$, the minimization is repeated for a value of $\hat{z}_*$ that is enlarged by a characteristic length of the problem—say, $\hat{z}_* + 1/\mathrm{Im}(\hat{\gamma}_*)$ instead of $\hat{z}_*$. Only if this second minimization yields a zero value of the cost function (up to numerical error) at a complex phase speed that is equal to the complex phase speed obtained in the first minimization (within sufficient accuracy, say, relative discrepancy smaller than 0.001) one can be certain to have found a correct solution of the eigenvalue problem.

The minimization of the cost function can be performed numerically using standard iterative techniques, for example, a quasi-Newton method (Gill et al. 1981), provided a moderately accurate guess for the complex eigenfrequency is available. But even without a good first guess, it is straightforward to search a large number of eigenfrequencies. Having found a solution for some particular parameter values, the solution branch can be traced through parameter space. The symmetries of the eigenvalue problem for certain parameter values mentioned above can be exploited to facilitate the computations. It proved sufficient to approximate the gradient of the cost function by finite differences but it may even be provided exactly using the method of adjoint equations.

3. Results and discussion

The IGW instability is a function of nondimensional rotation rate R, IGW amplitude a, instability orientation α, nondimensional instability horizontal wavenumber k_*, and localization parameter of the wave packet σ. It is impossible to investigate all IGW configurations; some choices of parameters have to be made. The width of the Gaussian envelope of the wave packet is taken to be equal to the vertical wavelength of the basic-state gravity wave throughout this paper: $\sigma = \lambda_0 = 2\pi/m_0$. In the center region, the envelope is then very similar to the envelope used by Dunkerton (1997). Three rep-

resentative values of the rotation rate have been considered, namely the high-frequency limit $R = 0$, an intermediate value ($R = 0.6$) and a low-frequency case ($R = 0.95$). For any of the three cases, the instability has been traced through the entire range of instability wavenumbers for a couple of IGW amplitudes. The parallel instability ($\alpha = 0°$), the transverse instability ($\alpha = 90°$), as well as two intermediate azimuths ($\alpha = 30°$ and $\alpha = 60°$) have been analyzed. The present study focuses exclusively on the most unstable instability mode. In many cases, there are several unstable modes. Expectedly, the most unstable mode is then usually not the one that exhibits strongest radiation, however, it is obviously always the physically most relevant one. For $\alpha = 90°$, the complex frequency of the fastest growing mode turned out to be purely imaginary in all examined cases. The modes of transverse instability therefore always have vanishing penetration ratio (cf. section 2c).

a. $R = 0$

For $R = 0$, instability is only possible for convectively supercritical IGW amplitudes. In Fig. 1, frequency, growth rate, and penetration ratio of the fastest growing instability mode as a function of instability wavenumber are shown for $R = 0$ and $a = 1.5$. Frequency and growth rate are indicated in dimensional units for a background static stability of $N_0^2 = 0.0004\ \mathrm{s}^{-2}$. The diagram of growth rates (Fig. 1b) is virtually identical to the results of Dunkerton (1997) who examined the same configuration. This demonstrates the weak dependence of the instability on the exact shape of the envelope of the wave packet. The preferred instability is transverse. Growth rate asymptotes to the maximum growth rate of convection $N_0\sqrt{a-1}$ as $k_* \to \infty$. The transverse instability is purely convective without horizontal-scale selection. For $\alpha = 60°$, results are very similar with slightly smaller growth rates at any k_*. The parallel instability exhibits a local maximum of growth rate at small instability wavenumber representing a mode that is significantly influenced by shear. This maximum is less distinct at $\alpha = 30°$. Negative static stability is not essential for the growth of this mode (Dunkerton 1997). It may be called a mode of hybrid shear-convective instability as it is present only at convectively supercritical IGW amplitudes but is essentially formed by shear instability. For large k_*, the instability becomes purely convective without scale selection for all azimuths. The modes of parallel instability at small k_* are characterized by a large absolute penetration ratio. The absolute penetration ratio decreases rapidly from $\alpha = 0°$ to $\alpha = 90°$. At large k_*, the modes are nonradiating for all azimuths. The relative maximum and the relative minimum of growth rate of the parallel instability do not manifest themselves as relative extrema in the penetration ratio. This is due to the cutoff behavior of the penetration ratio when the real part of the instability frequency exceeds the constant background Brunt–Väisälä frequency of $N_0 = 0.02\ \mathrm{s}^{-1}$. Physically, it reflects the phase speed condition of McIntyre and Weissman (1978).

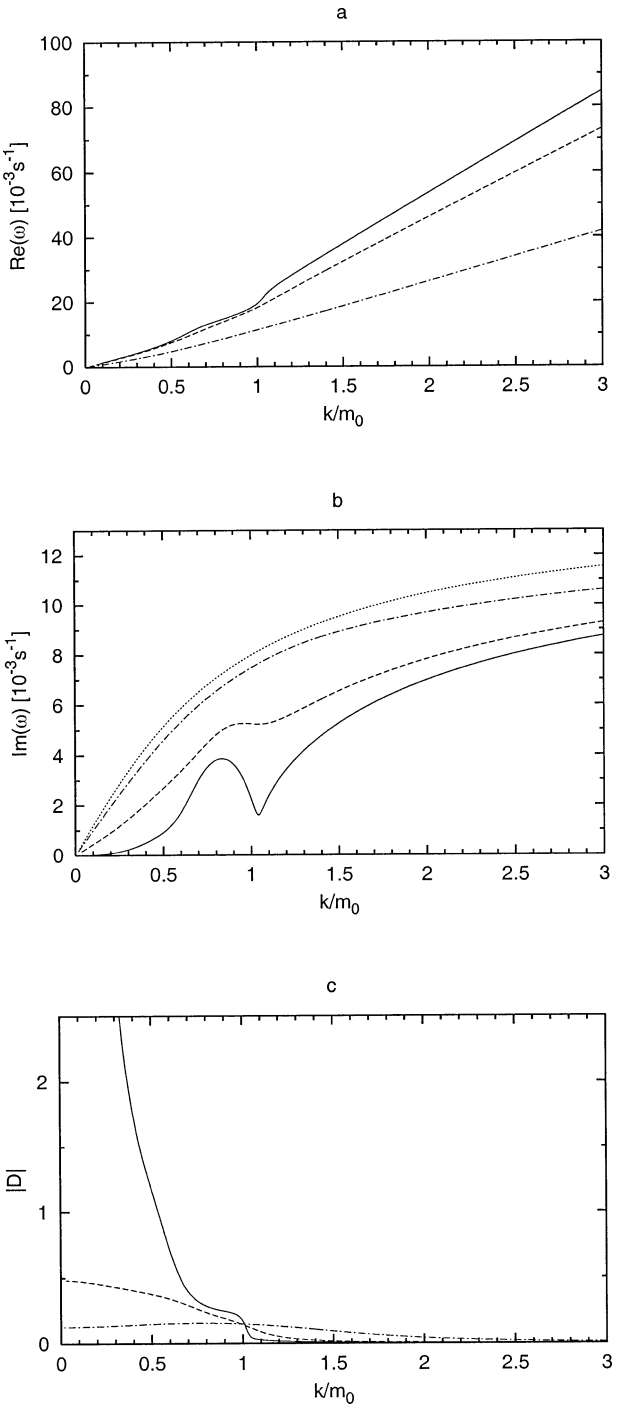

FIG. 1. Frequency (a), growth rate (b), and penetration ratio (c) of the fastest growing instability mode as a function of nondimensional instability wavenumber for $R = 0$ and $a = 1.5$. Azimuths are $\alpha = 0°$ (solid), $\alpha = 30°$ (dashed), $\alpha = 60°$ (dotted–dashed), and $\alpha = 90°$ (dotted). Constant background static stability is $N_0^2 = 0.0004\ \mathrm{s}^{-2}$.

Figure 2 illustrates the situation for $a = 1.1$. The

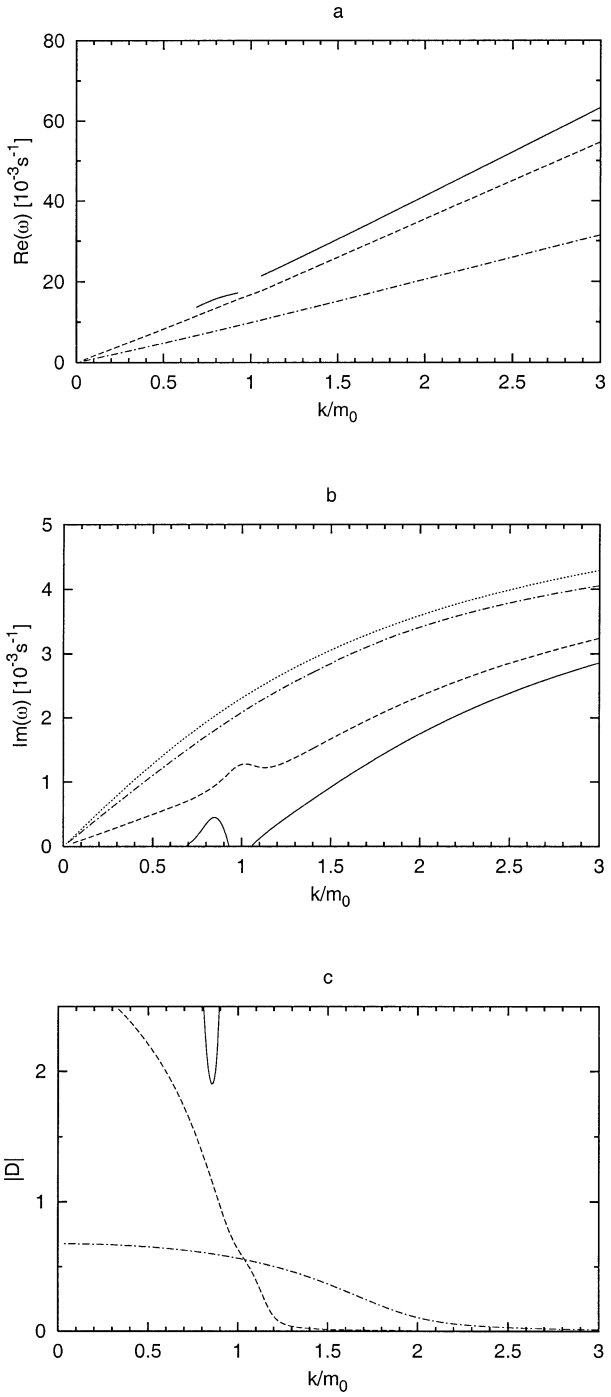

FIG. 2. Frequency (a), growth rate (b), and penetration ratio (c) as in Fig. 1, but for $R = 0$ and $a = 1.1$.

results remain qualitatively the same with growth rates considerably shifted to lower values and absolute penetration ratios considerably shifted to higher values. The cutoff at $\mathrm{Re}(\omega) = N_0$ acting at different wavenumbers for the different azimuths becomes even more clearly visible than with $a = 1.5$. At intermediate wavenumbers, the instability at $\alpha = 60°$ has a larger absolute penetration ratio than at $\alpha = 0°$ and $\alpha = 30°$, despite having a larger growth rate than those. Also, for small k_* where the frequencies are well below N_0 one clearly recognizes in both Fig. 1 and Fig. 2 that the penetration ratio does not merely reflect the growth rate but is substantially modified by the frequencies. Figure 3 displays the eigenfunction of the radiating mode of parallel instability for $a = 1.1$ at the wavenumber of maximum growth rate, namely $k_* = 0.85$, together with the corresponding profile of horizontal velocity. Also shown is the horizontally averaged vertical momentum flux associated with the instability given by $\langle\tilde{u}\tilde{w}\rangle \sim k_*[\mathrm{Re}(\phi_*')\,\mathrm{Im}(\phi_*) - \mathrm{Re}(\phi_*)\,\mathrm{Im}(\phi_*')]$, where $\tilde{u}$ and $\tilde{w}$ are the horizontal and vertical instability velocity, respectively, and the angle brackets denote the average over the horizontal coordinate. Moreover, the horizontally averaged generation of kinetic energy due to vertical shear given by $-\langle\tilde{u}\tilde{w}\rangle u_z \sim -k_*[\mathrm{Re}(\phi_*')\,\mathrm{Im}(\phi_*) - \mathrm{Re}(\phi_*)\,\mathrm{Im}(\phi_*')]u_*'$ is displayed. The eigenfunction attains its far-field behavior of free wave propagation at about $|z| = 2.3\lambda_0$. The penetration ratio is $D = -1.91$. The radiating character of the mode is clearly visible. The minima of the amplitude of the eigenfunction are located at the critical levels. The shear contribution to the generation of kinetic energy has large positive values in the region of instability. Hence, shear instability is the dominant physical mechanism behind this mode, independent of the fact that the basic state is also convectively unstable. The momentum flux decreases monotonically with increasing $|z|$ and has still considerable magnitude in the far-field regions as there are no critical levels outside the center of instability.

b. Intermediate R

At $R = 0.6$, instability still occurs only in convectively supercritical situations. The quantities characterizing the instability at $R = 0.6$ and $a = 1.3$ are shown in Fig. 4. There is a solution branch at small to intermediate wavenumbers for all azimuths. The growth rate increases from $\alpha = 0°$ to $\alpha = 90°$. The instability frequencies are smaller than N_0 for all azimuths. These modes exhibit strong horizontal-scale selection. They have large values of absolute penetration ratio that decrease from $\alpha = 0°$ to $\alpha = 90°$. As an example, the eigenfunction of parallel instability at the wavenumber of largest growth rate ($k_* = 0.84$) is shown in Fig. 5. The far-field regions begin at about $|z| = 1.7\lambda_0$. The penetration ratio is $D = -1.15$. Substantial radiation from the center of instability into the outer regions is present. The structure of the eigenfunction is similar to that in Fig. 3. The minima of the amplitude at the critical levels are more pronounced. Thus, the inner region is narrower in this example. Also the vertical momentum flux and the shear contribution to kinetic energy generation show similar behavior as in Fig. 3, but the decay in the outer regions is faster. Again, the mode is essentially due to shear instability. This mode has a growth

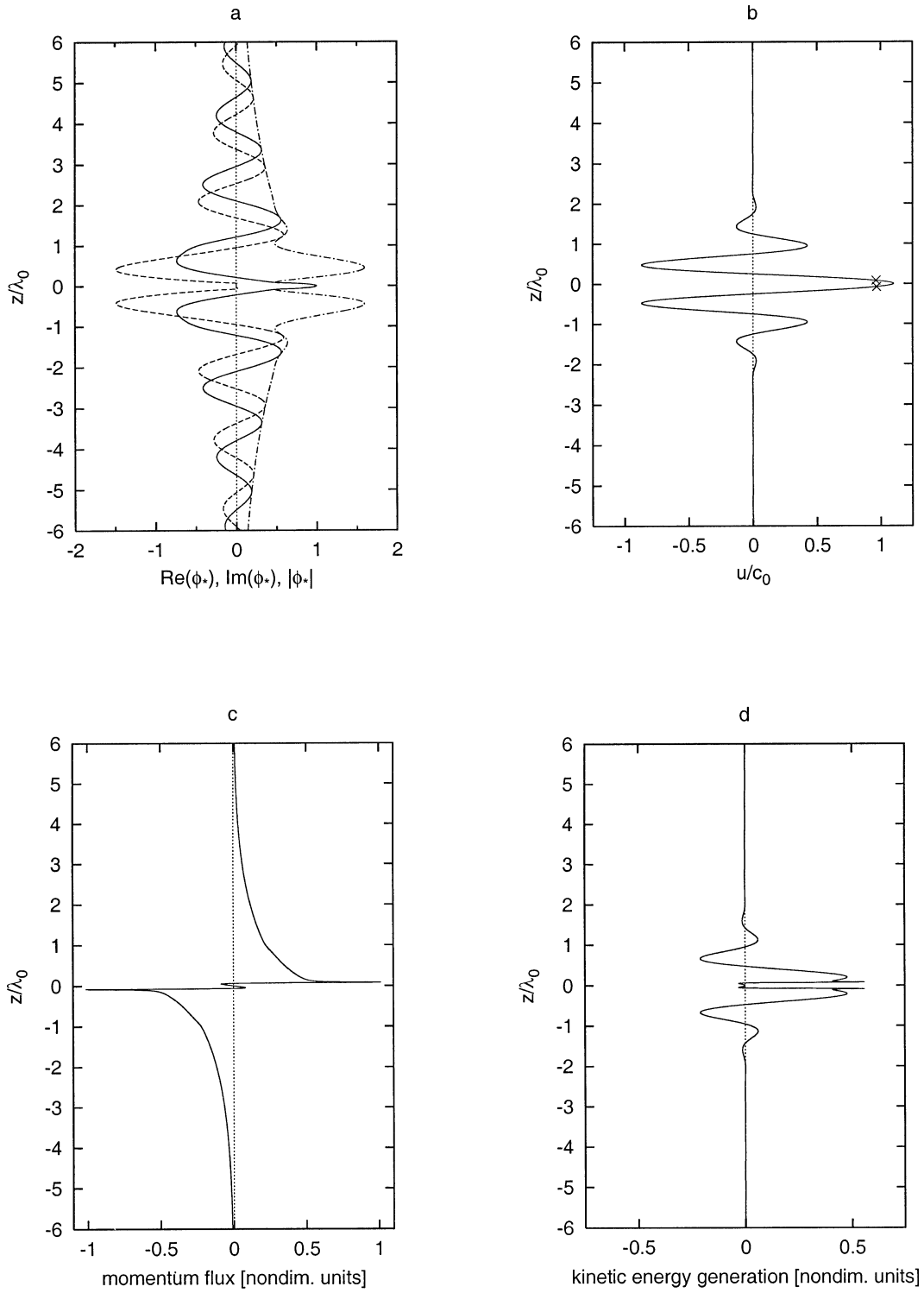

FIG. 3. Real part (solid), imaginary part (dashed), and amplitude (dotted–dashed) of the fastest growing instability mode (a), velocity profile (b), horizontally averaged vertical momentum flux (c), and generation of kinetic energy due to shear (d) for $R = 0$, $a = 1.1$, $\alpha = 0°$, and $k_* = 0.85$. Crosses in (b) indicate critical levels. Penetration ratio is $D = -1.91$.

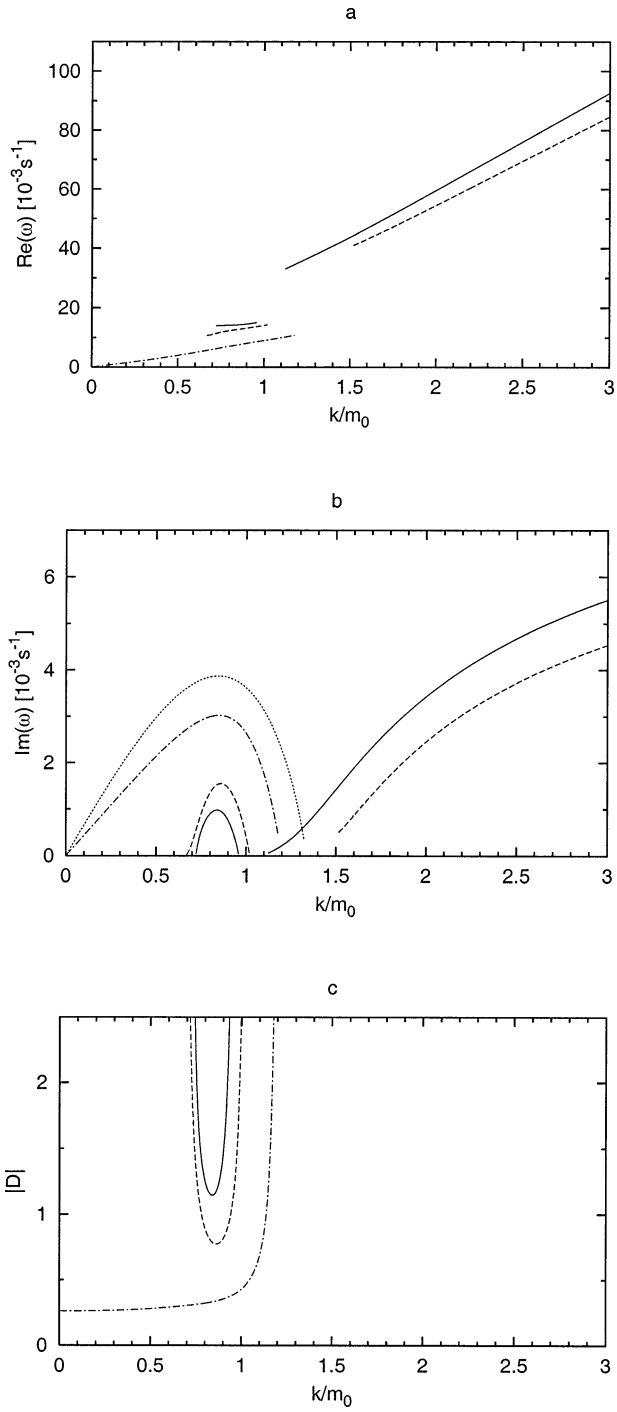

FIG. 4. Frequency (a), growth rate (b), and penetration ratio (c) as in Fig. 1, but for $R = 0.6$ and $a = 1.3$.

rate of 0.000 978 s^{-1}. The largest absolute penetration ratio that is possible for an instability of this growth rate with arbitrary profiles of horizontal velocity and static stability in the center region is 1.25 (cf. section 2b). Interestingly, this value is almost reached by the IGW configuration considered here. At larger k_*, there are branches of purely convective instability for $\alpha = 0°$ and $\alpha = 30°$. Growth rates for $\alpha = 30°$ are smaller than for $\alpha = 0°$. These convective modes have almost zero penetration ratio as their frequencies lie well above N_0. For $\alpha = 60°$ and $\alpha = 90°$, these convective branches are completely suppressed.

c. $R \to 1$

For low-frequency gravity waves—that is, $R \to 1$—shear instability takes precedence over convective instability. In Fig. 6, the instability is displayed for $R = 0.95$ and $a = 1.1$. Growth rate depends only weakly on azimuth (cf. Dunkerton 1997). The modes are clearly dominated by shear instability with distinct horizontal-scale selection even at convectively supercritical IGW amplitude. The frequencies are well below N_0 in the whole range of wavenumbers. At the wavenumber of maximum growth rate, the modes have a very small absolute penetration ratio.

Figure 7 illustrates a convectively subcritical situation, that is, a case of pure shear instability, namely $R = 0.95$ and $a = 0.7$. The band of wavenumbers exhibiting instability becomes narrower. The growth rates decrease distinctly compared to the case with $a = 1.1$; the dependence of the growth rate on azimuth becomes much stronger than with $a = 1.1$. Figure 8 gives the eigenfunction of the parallel instability at the wavenumber of maximum growth rate ($k_* = 0.85$). The far-field regime is reached at about $|z| = 1.2\lambda_0$. The penetration ratio is $D = -1.00$. Here, a limitation of the penetration ratio as an indicator of radiation becomes visible. The mode has a relatively large value of $|D|$ (only slightly smaller than that of the mode in Fig. 5), and a zoomed view of the mode for $|z| > 1.2\lambda_0$ (not shown) does indeed reveal that the mode is characterized in the far-field regions by a slowly decreasing amplitude. However, the amplitude of the eigenfunction has already decreased to negligible values before reaching the far-field regime. The eigenfunction and the momentum flux sharply decrease to zero at the critical levels at about $\pm 0.85\lambda_0$. Right in front of the critical levels, there are regions in which an increase of kinetic energy of the primary wave takes place. Such behavior is completely in line with the well known phenomenon of a linearly propagating wave that approaches a critical level and is not able to pass it (Lighthill 1978). Hence this mode is from a physical point of view clearly a nonradiating one. We conclude that a large absolute penetration ratio can only be taken as an indicator of radiation if there are no critical levels outside the region in which the instability is effectively generated. Configurations with critical levels close to the far-field regions are not able to radiate.

Additionally to the representative examples shown so far, Fig. 9 gives a summarizing overview on parameter space for $\alpha = 0°$, where most radiating modes occur. The regions of instability and large absolute penetration

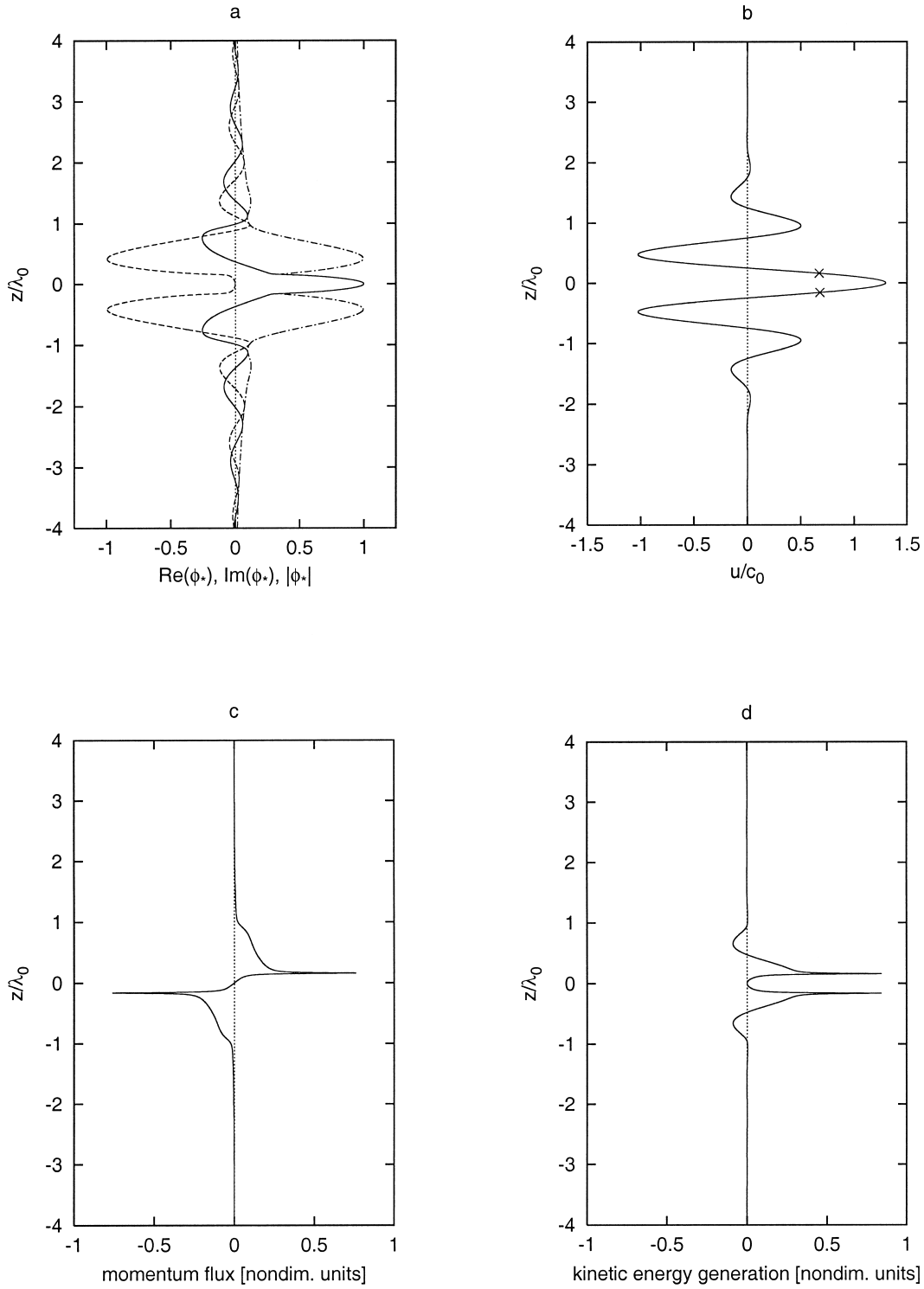

FIG. 5. Eigenfunction (a), velocity profile (b), vertical momentum flux (c), and kinetic energy generation due to shear (d) as in Fig. 3, but for $R = 0.6$, $a = 1.3$, $\alpha = 0°$, and $k_* = 0.84$. Penetration ratio is $D = -1.15$.

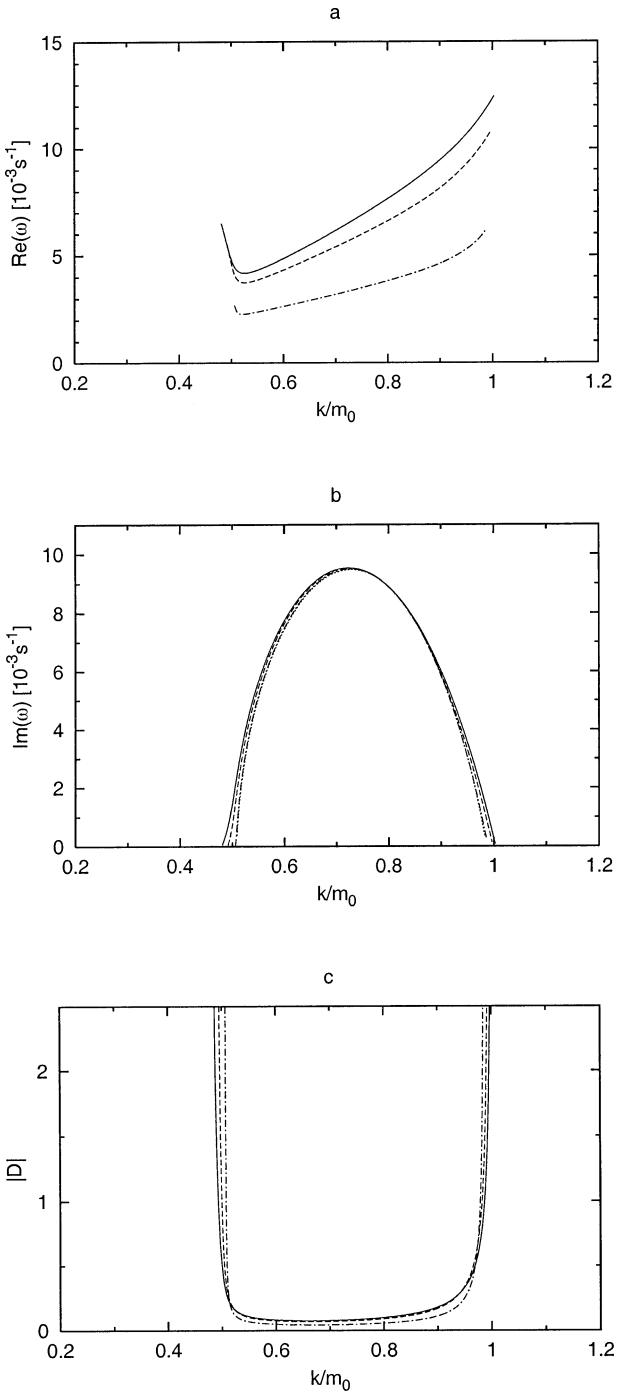

FIG. 6. Frequency (a), growth rate (b), and penetration ratio (c) as in Fig. 1, but for $R = 0.95$ and $a = 1.1$.

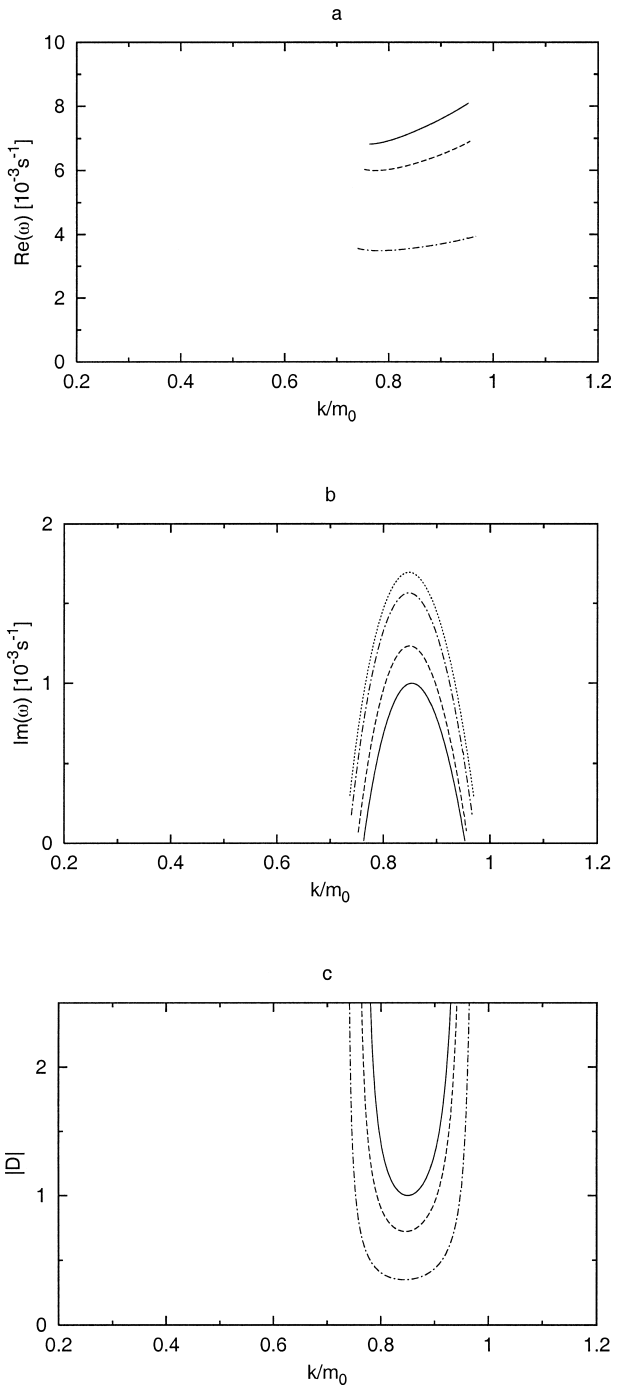

FIG. 7. Frequency (a), growth rate (b), and penetration ratio (c) as in Fig. 1, but for $R = 0.95$ and $a = 0.7$.

ratio are indicated in the k_*–a plane for the three considered values of R. Here, $|D| = 1$ (decrease of the amplitude of the instability eigenfunction in the far-field regions by a factor e within a wavelength) is a natural threshold value to classify modes as radiating or nonradiating, respectively. At $R = 0$, there is a region of shear instability extending from intermediate to small instability wavenumbers. These modes have a large absolute penetration ratio if the basic-state amplitude is not too large. All instability modes at $R = 0$ have no critical levels outside the very region of instability (as in the example in Fig. 3), and inspection of the eigenfunctions shows that all modes with large absolute penetration ratio are indeed radiating. A domain of non-

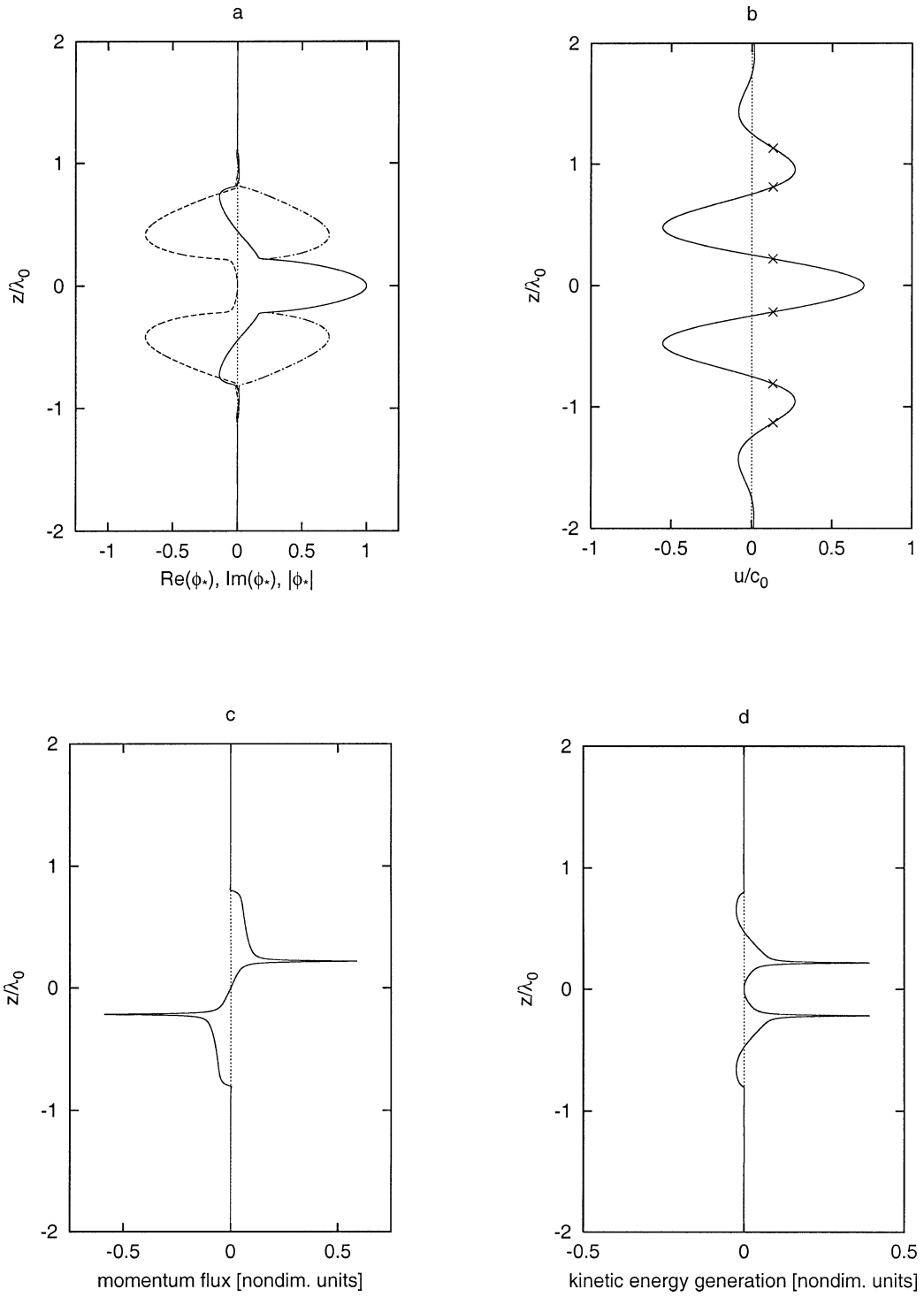

FIG. 8. Eigenfunction (a), velocity profile (b), vertical momentum flux (c), and kinetic energy generation due to shear (d) as in Fig. 3, but for $R = 0.95$, $a = 0.7$, $\alpha = 0°$, and $k_* = 0.85$. Penetration ratio is $D = -1.00$.

radiating modes of convective instability reaches from intermediate to infinitely large instability wavenumbers. The overall picture for $R = 0.6$ is very similar to that for $R = 0$. The regions of shear and convective instability are now separated; larger basic-state amplitudes are required for shear instability to set in. Again, for all modes, only a single pair of critical levels in the center region occurs and the modes with large absolute pen-

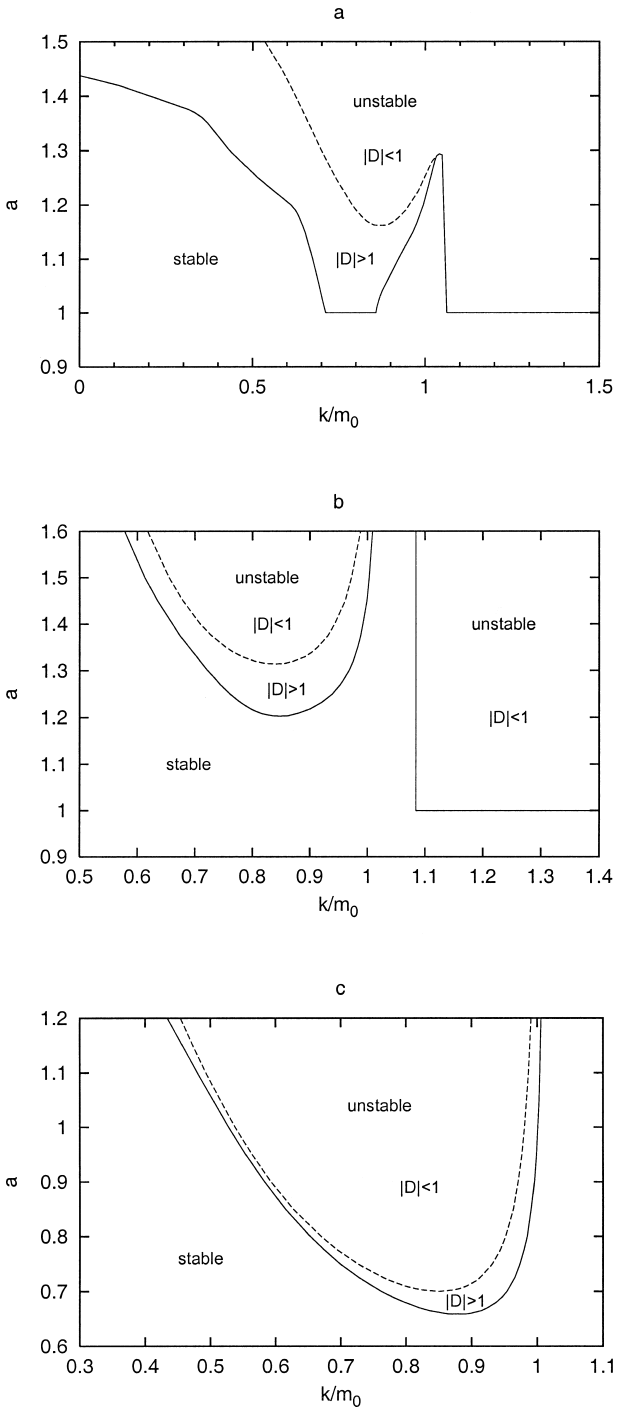

FIG. 9. Neutral curves (solid) and isoline $|D| = 1$ of the fastest growing mode (dashed) in the case $\alpha = 0°$ for $R = 0$ (a), $R = 0.6$ (b), and $R = 0.95$ (c).

etration ratio are radiating. At $R = 0.95$, convective instability is suppressed. Shear instability sets in at intermediate instability wavenumbers already for convectively subcritical amplitudes. Part of these shear modes possess a large absolute penetration ratio. However, all instabilities at $R = 0.95$ have further critical levels outside the center of instability as already shown for the example $k_* = 0.85$ and $a = 0.7$ (cf. Fig. 8 and the corresponding discussion above). The eigenfunctions and the corresponding momentum fluxes and kinetic energy generation terms show that even the instabilities with large absolute penetration ratios are nonradiating.

The question as to the physical importance of radiating instabilities as a mechanism for gravity wave breakdown and generation of turbulence rises. On the one hand, for all IGW configurations that support radiating instabilities, there are nonradiating instabilities at larger horizontal wavenumbers and/or other azimuths having larger growth rates than the radiating modes. This seems to limit the role of the radiating modes. On the other hand, there are some points in favor of a dominant role of radiating instabilities. First, Dunkerton and Robins (1992) have found in a nonlinear simulation of a gravity wave critical layer that radiating modes at intermediate wavenumbers can grow to considerable amplitude prior to nonradiating modes at large wavenumbers, despite having a smaller growth rate within linear theory. They attribute this to a nonlinear cascade of energy causing intermediate instability wavenumbers to grow first. Second, instabilities at large wavenumbers that are always nonradiating will be suppressed in model simulations due to scale-selective horizontal diffusion, thus stressing the radiating modes compared to the nonradiating ones. Finally, the fact that strong turbulence in the mesosphere does not necessarily occur in regions of most unstable conditions (Lübken et al. 1994) suggests the possibility of an important role of radiating modes provided local instability is the dominant mechanism in the generation of turbulence at all. A treatment of the problem by means of nonlinear simulation at high resolution in a domain large enough to encompass significant radiation would be most interesting to shed light on all these issues.

4. Summary and conclusions

The vertical radiation of local convective and shear instabilities arising from internal inertio-gravity waves (IGW) has been examined within linear stability theory. A steady, plane-parallel Boussinesq flow with vertical profiles of horizontal velocity and static stability resembling an IGW packet without mean vertical shear has been used as a dynamical framework. The influence of frequency and amplitude of the primary gravity wave, as well as orientation and horizontal wavenumber of the instability on vertical radiation, has been investigated by tracing the instability for a couple of representative IGW configurations. The radiation of an instability mode is measured by the extent to which the eigenfunction penetrates from the region of instability into the adjacent stable regions of the wave field as given by the penetration ratio. Radiating modes have been found at small to intermediate instability wavenumbers for basic-state gravity waves with high to intermediate

frequencies and moderately convectively supercritical amplitudes. Radiation is then strongest when the horizontal wavevector of the instability is aligned parallel to the horizontal wavevector of the basic-state gravity wave. Transverse instabilities are always nonradiating. The radiating modes are modes of hybrid shear–convective instability since they only exist under convectively supercritical conditions but clearly appear to be shaped by shear instability. Convective instabilities that are found at large instability wavenumbers or strongly convectively supercritical amplitudes, as well as shear instabilities of low-frequency basic-state gravity waves, are nonradiating. The radiation of an instability is related to the existence of critical levels. A mode is able to radiate only if there are no critical levels outside the region of instability of the primary gravity wave.

The physical importance of the radiating instabilities versus the nonradiating ones in gravity wave saturation and generation of turbulence certainly cannot be finally assessed on the basis of the linear stability analyses presented here. The question as to the extent to which linear theory is reliable in each of the different examined situations remains. Nonlinear high-resolution numerical simulations of the different IGW configurations may provide valuable further information.

REFERENCES

Drazin, P. G., and W. H. Reid, 1981: *Hydrodynamic Stability*. Cambridge University Press, 525 pp.

Dunkerton, T. J., 1997: Shear instability of internal inertia-gravity waves. *J. Atmos. Sci.*, **54,** 1628–1641.

——, and R. E. Robins, 1992: Radiating and nonradiating modes of secondary instability in a gravity-wave critical layer. *J. Atmos. Sci.*, **49,** 2546–2559.

Fritts, D. C., and P. K. Rastogi, 1985: Convective and dynamical instabilities due to gravity wave motions in the lower and middle atmosphere: Theory and observations. *Radio Sci.*, **20,** 1247–1277.

——, and L. Yuan, 1989: Stability analysis of inertio-gravity wave structure in the middle atmosphere. *J. Atmos. Sci.*, **46,** 1738–1745.

Gill, P. E., W. Murray, and M. H. Wright, 1981: *Practical Optimization*. Academic Press, 401 pp.

Howard, L. N., 1961: Note on a paper by John W. Miles. *J. Fluid Mech.*, **10,** 509–512.

Lelong, M.-P., and T. J. Dunkerton, 1998a: Inertia-gravity wave breaking in three dimensions. Part I: Convectively stable waves. *J. Atmos. Sci.*, **55,** 2473–2488.

——, and ——, 1998b: Inertia-gravity wave breaking in three dimensions. Part II: Convectively unstable waves. *J. Atmos. Sci.*, **55,** 2489–2501.

Lighthill, M. J., 1978: *Waves in Fluids*. Cambridge University Press, 504 pp.

Lübken, F.-J., and Coauthors, 1994: Morphology and sources of turbulence in the mesosphere during DYANA. *J. Atmos. Terr. Phys.*, **56,** 1809–1833.

McIntyre, M. E., and M. A. Weissman, 1978: On radiating instabilities and resonant overreflection. *J. Atmos. Sci.*, **35,** 1190–1196.

Miles, J. W., 1961: On the stability of heterogeneous shear flows. *J. Fluid Mech.*, **10,** 496–508.

Sutherland, B. R., and W. R. Peltier, 1994: Turbulence transition and internal wave generation in density stratified jets. *Phys. Fluids*, **6,** 1267–1284.

——, C. P. Caulfield, and W. R. Peltier, 1994: Internal gravity wave generation and hydrodynamic instability. *J. Atmos. Sci.*, **51,** 3261–3280.

Walterscheid, R. L., and G. Schubert, 1990: Nonlinear evolution of an upward propagating gravity wave: Overturning, convection, transience, and turbulence. *J. Atmos. Sci.*, **47,** 101–125.

Winters, K. B., and E. A. d'Asaro, 1989: Two-dimensional instability of finite amplitude internal gravity wave packets near a critical level. *J. Geophys. Res.*, **94,** 12 709–12 719.

Yuan, L., and D. C. Fritts, 1989: Influence of a mean shear on the dynamical instability of an inertio-gravity wave. *J. Atmos. Sci.*, **46,** 2562–2568.